RAA 2018 Vol. **18** No. **7**, 74(10pp) doi: 10.1088/1674–4527/18/7/74

http://www.raa-journal.org *http://iopscience.iop.org/raa*

***R**esearch in*
***A**stronomy and*
***A**strophysics*

Investigation of the possible source for the solar energetic particle event on 2017 September 10

Ming-Xian Zhao[1], Gui-Ming Le[1,2] and Yu-Tian Chi[3]

[1] Key Laboratory of Space Weather, National Center for Space Weather, China Meteorological Administration, Beijing 100081, China; *Legm@cma.gov.cn*

[2] School of Computer Science, Anhui University of Technology, Ma'anshan 243032, China

[3] School of Earth and Space Sciences, University of Science and Technology of China, Hefei 230026, China

Received 2018 January 12; accepted 2018 March 16

Abstract According to the solar proton data observed by *Geostationary Operational Environmental Satellites* (*GOES*), ground-based neutron monitors on Earth and near-relativistic electron data measured by the *ACE* spacecraft, the onset times of protons with different energies and near-relativistic electrons have been estimated and compared with the time of solar soft and hard X-ray and radio burst data. The results show that first arriving relativistic and non-relativistic protons and electrons may have been accelerated by the concurrent flare. The results also suggest that release times of protons with different energies may be different, and the protons with lower energy may have been released earlier than those with higher energy. Some protons accelerated by concurrent flares may be further accelerated by the shock driven by the associated CME.

Key words: Sun: coronal mass ejections (CMEs) — Sun: flares — Sun: particle emission

1 INTRODUCTION

A large gradual solar energetic particle (SEP) event is often accompanied by both a gradual flare and coronal mass ejection (CME). Whether a gradual flare contributes to the production of protons in a large gradual SEP event is still an open question. The results of some papers suggested that relativistic solar protons (RSPs) may be accelerated by concurrent flares (e.g., Aurass et al. 2006; Bazilevskaya 2009; Grechnev et al. 2008, 2015; Klein et al. 2014; Kouloumvakos et al. 2015; Le et al. 2006, 2013, 2014, 2016; Li et al. 2007a,b, 2009; Masson et al. 2009; Miroshnichenko et al. 2005b; Pérez-Peraza et al. 2009; Simnett 2006). A simple and effective method is to calculate the release time of RSPs and compare it with the time of the concurrent flare and metric Type II radio burst, and then the solar origin of the first arriving particles can be judged. The release times for many ground level enhancement (GLE) events inferred from velocity dispersion analysis (VDA) seemly support that RSPs may be accelerated by a CME-driven shock (Reames 2009b,a). The path length for protons propagating from the Sun to the Earth inferred by VDA is usually much longer than the nominal Parker spiral line. It can be noticed that the release time for some GLE event obtained by different researchers may be different. For example, the solar origin of RSPs in the SEP event from 2003 October 28 obtained by Miroshnichenko et al. (2005b) is different from the one obtained by Reames (2009b). The possible sources for non-relativistic protons have also been investigated and the results showed that $E > 30\,\mathrm{MeV}$ protons may be mainly accelerated by concurrent flares for SEP events with source location in the longitudinal area ranging from W40 to W70 (Le et al. 2017; Le & Zhang 2017). When a large gradual SEP happens, near relativistic electrons and even relativistic electrons are often accompanied by a long lasting and intense Type III burst. The long lasting and very intense Type III burst is termed a Type III-l burst (Cane et al. 2002). The origins of near relativistic electrons and

relativistic electrons have been extensively investigated and different researchers have different points of view on the origin of the near-relativistic electrons (e.g., Cane et al. 2002, 2006, 2010; Cane 2003; Kahler et al. 2007; Cliver & Ling 2009 and reference therein). The conclusion that near relativistic electrons or higher energy electrons undergo shock acceleration is based on the assumption that the path length traveled by near relativistic electrons from the Sun to the Earth is 1.2 AU.

An X8.2 flare that occurred on 2017 September 10 was accompanied by a very fast CME. Protons escaped from the Sun with energies from keV to GeV and near relativistic electrons were observed. According to the RSP data observed by neutron monitors (NMs) and *GOES* spacecraft, and the near-relativistic electrons observed by the *ACE* spacecraft, as well as solar soft and hard X-ray (HXR) and radio burst data, solar release times (SRTs) of protons and electrons with different energies that occurred on 2017 September 10 will be estimated and then compared with the flare time and the metric Type II radio burst onset time to speculate the possible solar source for protons with different energies. This is the motivation of this paper. Data observation is described in Section 2. Data analysis is provided in Section 3. Discussion and summary are presented in Section 4.

2 OBSERVATION DATA

Active region (AR) 12673 located at S08W88 produced an X8.2 flare. This flare started at 15:35 UT, peaked at 16:06 UT and ended at 16:31 UT on 2017 September 10. The onset time of the metric Type III burst, as observed by *STEREO-A*, is 15:48 UT, as shown in Figure 1. HXR with energy 100–300 keV peaked at 15:56 UT, while HXR with energy 300–1000 keV peaked at 15:59:30 UT on 2017 September 10. The flare was accompanied by a very fast CME. The CME entered the Large Angle and Spectrometric Coronagraph (LASCO) C2 and C3 field of view at 16:00 UT and 16:06 UT on 2017 September 10 respectively. The onset time of the Type II radio burst generated by the shock driven by the fast CME is slightly later than 16:03 UT, 2017 September 10, as obtained from e-Callisto (*http://e-callisto.org/*) which is shown in Figure 2.

The flux of protons with different energies observed by *GOES* increased very quickly after the X8.2 flare as displayed in Figure 3.

A standard deviation, δ, calculated by the formula below, will be used to estimate the onset time of first arriving particles

$$\delta = \sqrt{\sum_{i=1}^{N} (x_i - \overline{x})^2 / N}\,, \tag{1}$$

where x_i and $\overline{x}$ are the real and averaged value during the quiet period. N is the number of measurements (experimental records) during the quiet period. The estimation of the onset time for first arriving particles is based on the intensity of particles exceeding $\overline{x} + 2\delta$ (e.g., Mewaldt et al. 2003; Tylka et al. 2003; Miroshnichenko et al. 2005a). Using this criterion, we can obtain the onset times of first arriving particles from the data observed by *GOES* or by other instruments.

$$t_{\rm s} = t_{\rm o} - L/v\,, \tag{2}$$

where $t_{\rm s}$ is the release time on the Sun, while $t_{\rm o}$ is the onset time of particles observed in situ, such as observed by *GOES* or by NMs on the ground.

The onset time estimated for $E > 700$ MeV protons is 16:15 UT$\pm$5 min, while the onset time estimated for $E > 10$ MeV protons is 16:25 UT$\pm$5 min. However, the onset times estimated for $E > 30$ MeV protons, $E > 50$ MeV protons and $E > 100$ MeV protons are 16:20 UT$\pm$5 min.

The GLE event caused by the interaction between RSPs and the atmosphere was observed by several NMs and are plotted in Figure 4. According to formula (1), the onset time for each NM displayed in Figure 4 has been estimated and is listed in Table 3. In fact, all NMs at Earth's surface with geomagnetic cutoff rigidities below 1 GV have the same cutoff (about 1 GV), which is only determined by atmospheric absorption (e.g., Miroshnichenko 2001; Bieber et al. 2002). The different arrival times for RSPs suggest that there was a very strong anisotropy in RSPs at the early phase of the SEP event. The onset time registered by the FMST NM with cutoff rigidity 1.0 GV is earlier than that registered by MDGN NM with cutoff rigidity 2.09 GV, suggesting that RSPs with higher energy may be released later than RSPs with lower energy. We can also see from Figure 4 that the enhancement in cosmic rays observed by Newk, which has a cutoff rigidity 2.4 GV, is not obvious, suggesting that few protons have energy higher than than 1.64 GeV.

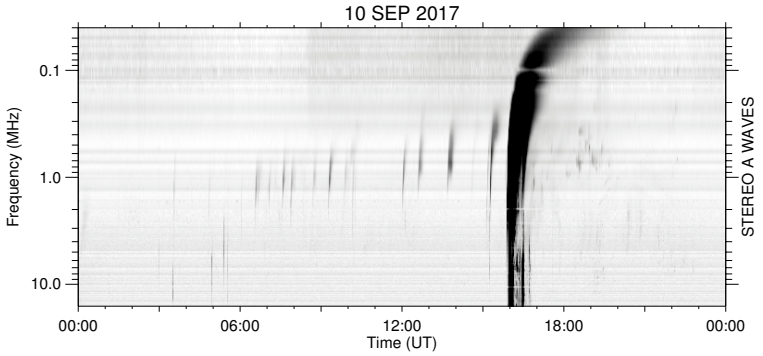

Fig. 1 Type III radio burst associated with the large SEP event on 2017 September 10.

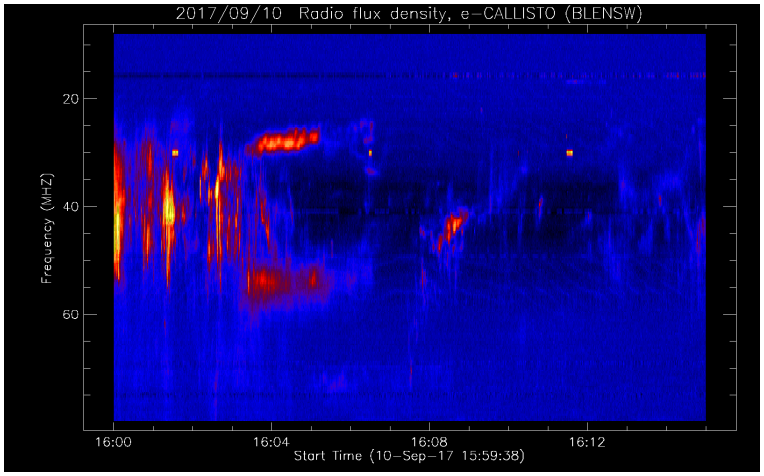

Fig. 2 Metric Type II radio burst associated with the SEP event on 2017 September 10.

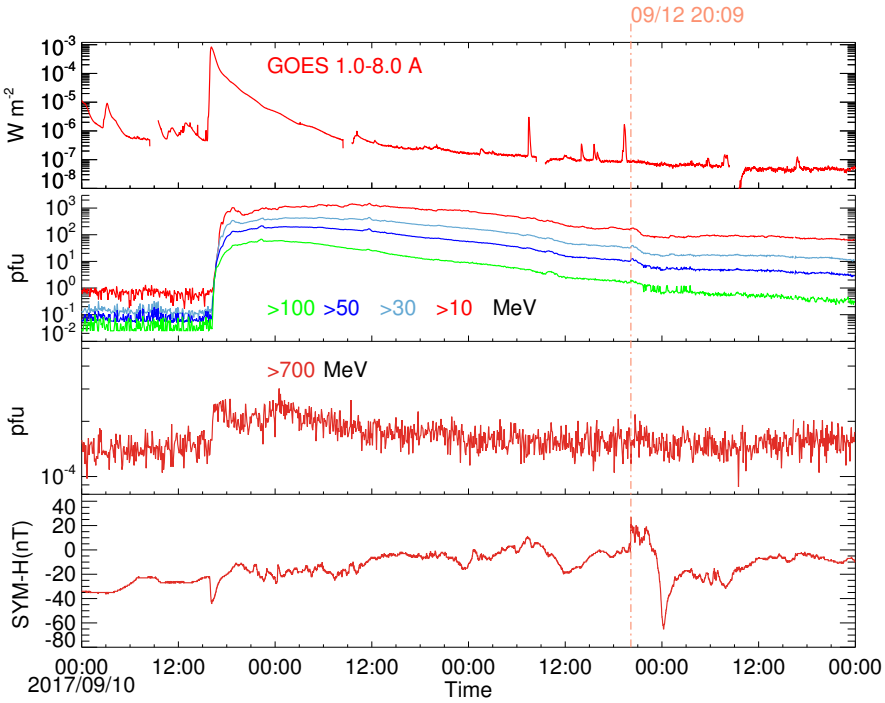

Fig. 3 The SXR emission and the fluxes of protons with different energies varied with time on 2017 September 10. From top to bottom, the panels indicate the flux of SXR in 1–8 Å, flux of protons with different energies ($E > 10$, 30, 50 and 100 MeV protons), flux of $E > 700$ MeV protons and 1-minute time resolution SYM-H index.

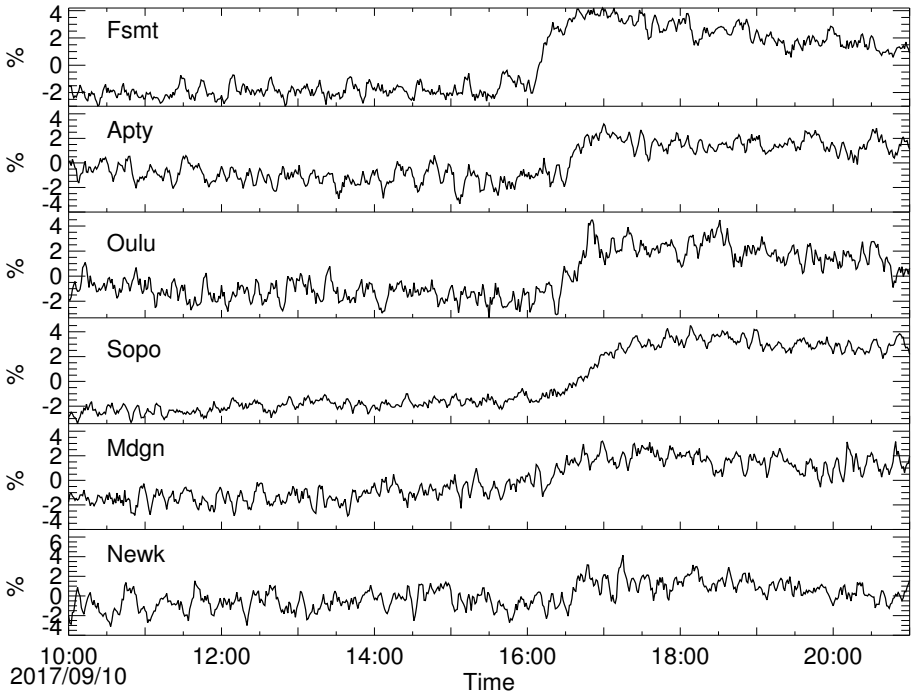

Fig. 4 The GLE event observed by several NMs on 2017 September 10.

3 DATA ANALYSIS

3.1 Estimation of the Path Length Traveled by SEPs

Type III bursts are caused by streams of electrons with energy lower or higher than 25 keV. The presence of a metric type and lower frequency Type III burst indicates that the field lines over the associated active region have been opened and the particles escape into interplanetary space. The onset time of the Type III radio burst displayed in Figure 1 is 10 min later than the start time of the X8.2 flare. The Type III radio burst exhibited in Figure 1, which lasted tens of minutes, is a typical Type III-l burst. Different people have different points of view on the origin of Type III-l bursts and their relationship with large gradual SEP events (e.g., Cane et al. 2002, 2006, 2010; Cane 2003; Cliver & Ling 2009; Kahler et al. 2007 and references therein). The start time of the Type III-l burst shown in Figure 1 is 15:48 UT, 15 min earlier than the start time of the Type II burst shown in Figure 2, suggesting that it is impossible that the electrons responsible for the Type III-l burst were accelerated by CME-driven shock. The release times of near relativistic electrons inferred from VDA are almost always delayed relative to the start times of the associated Type III-l radio burst and even in the small electron events in which electrons were believed to be accelerated by concurrent flares (Cane & Lario 2006). It has been known that electrons can be efficiently accelerated in solar flares (Lin et al. 2003). The start time of the Type III-l burst can be treated as the SRT of electrons. Based on the time difference between the start time of the Type III-l burst and the onset time of 38–53 keV electrons observed by the *ACE* spacecraft, the path length traveled by electrons with energy 38–53 keV is estimated as $\sim 1.7\pm0.22$ AU. According to the path length $\sim 1.7\pm0.22$ AU, the SRT of near-relativistic electrons with energies 173–315 keV was about 15:48:42 ST$\pm$5 min, which is consistent with the first peak time of 100–300 keV HXR shown in Figure 5. The fluxes of HXR in three channels shown in Figure 5 are obtained from the *Fermi* Gamma Ray Burst Monitor (Meegan et al. 2009).

3.2 Estimated CME and CME-driven Shock Speed

By using coronagraph images taken by SECCHI/COR2 instruments onboard the *STEREO-A* and *STEREO-B* spacecraft and the LASCO suite (Brueckner et al. 1995) onboard the *Solar and Heliospheric Observatory* (*SOHO*), three dimensional CMEs can be modeled

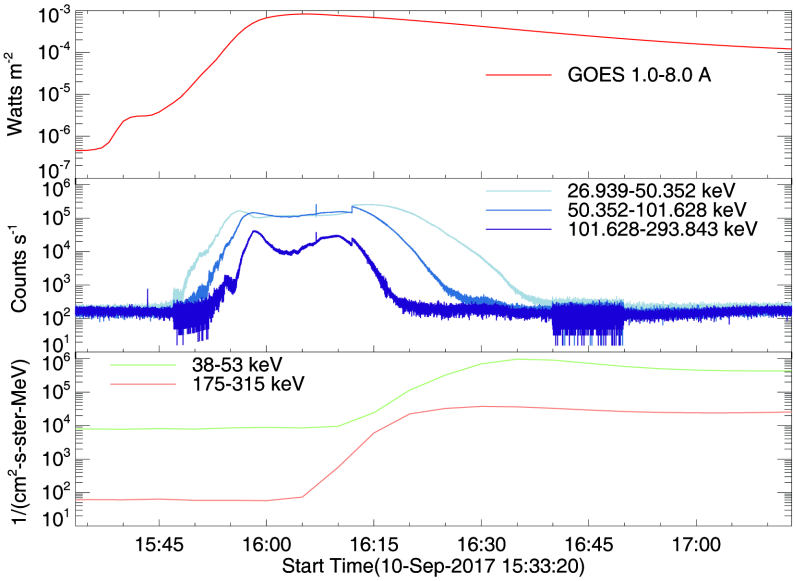

Fig. 5 The SXR emission and the fluxes of electrons with two energy channels. From *top* to *bottom*, the panels indicate the flux in 1–8Å, HXR flux in three channels and flux of near relativistic electrons in two channels respectively.

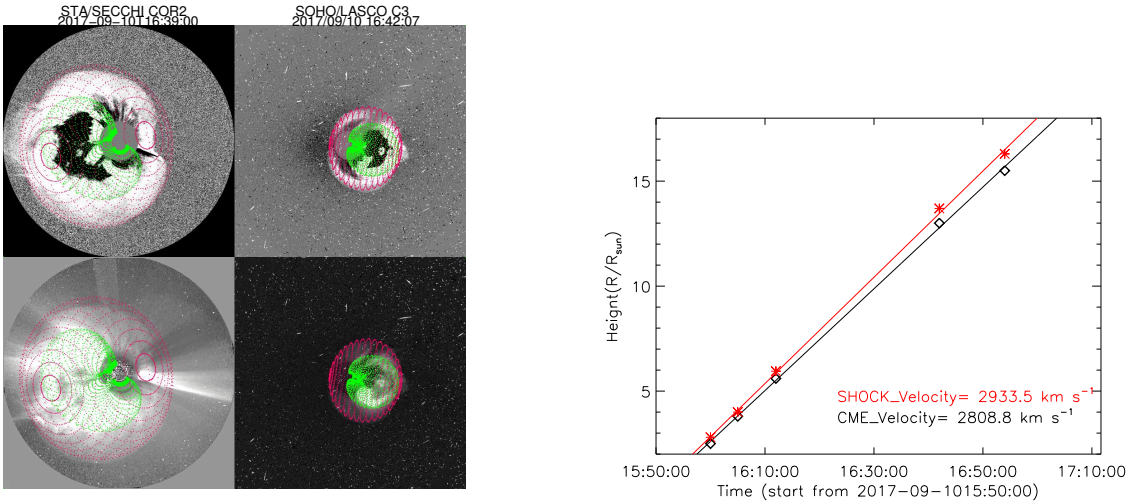

Fig. 6 Model fitting of CME front and shock front. *Left*: The *green mesh* shows the GCS fitting to the CME and the *red mesh* represents the spheroid fitting to the shock front. The linear fit of CME front height (*black*) and shock front height (*red*) to time is shown in the right image.

with the Graduated Cylindrical Shell (GCS) model (Thernisien et al. 2006, 2009) from the low corona to 1 AU. As communications to *STEREO-B* have been interrupted since 2014 October 1, we only use coronagraph images from *SOHO*/LASCO and *STEREO-A* to reconstruct this CME. The shape of the GCS flux rope model is reminiscent of a hollow croissant and can be parameterized with six free parameters. These six parameters are Carrington longitude Φ, heliospheric latitude θ, tilt angle γ, the leading front edge distance of the tracked structure from the Sun $h_{\rm front}$, the half angle of the shell α and the aspect ratio κ. There is also a spheroid model that can be applied to reconstruct the shock with six free parameters, longitude, latitude, tilt angle, height, and the major and minor axes of the spheroid (ε and κ).

In this article, we focus on the velocity of the CME and shock, so the height of flux rope front and the height of the shock front are mainly considered. The CME flux rope structure can be seen more clearly in direct images (Fig. 6 bottom-left panels), while the shape of the shock

is more clear in running difference images (Fig. 6 top-left panels). As shown in the four left panels of Figure 6, the red overlaid mesh (spheroid model) shows the CME shock front and the green mesh (GCS model) represents the CME flux rope front. After successfully fitting the flux rope model and spheroid shock model with a series of COR2 and C3 images at different times, a set of height-time data will be obtained. All fitting parameters of the GCS model are listed in Table 1 and the spheroid model parameters for the shock are provided in Table 2. The velocity of the CME flux rope front and shock front can be derived after the linear fitting of height and time. The height-time fitting results are displayed in the right panel of Figure 6. The fitted CME speed is about 2808.8 km s^{-1}, while the CME-driven shock speed is around 2933.5 km s^{-1}.

3.3 Release Times

The relationship between the kinetic energy and rigidity, and the relationship between the speed and kinetic energy of a particle can be described by the two formulas (Le et al. 2006) listed below

$$\begin{aligned} E_{\rm k} &= \frac{-2E_0 + \sqrt{(E_0)^2 + (ZeR)^2}}{2}, \\ v &= \frac{\sqrt{E_{\rm k}^2 c^2 + 2E_{\rm k} m_0 c^4}}{E_{\rm k} + E_0}, \end{aligned} \tag{3}$$

where R is the particle rigidity, Z is the particle charge number and e is the charge of an electron, $E_{\rm k}$ is the particle's kinetic energy while E_0 is the particle's rest energy. c is the light speed and m_0 is the rest mass of the particle.

According to formula (3), we can obtain the speed of a particle with kinetic energy $E_{\rm k}$. When the path length traveled by particles is known, the SRTs of protons with different energies can be derived according to formula (2). The time information for particles with different energies is listed in Table 3.

4 DISCUSSION AND SUMMARY

The VDA has three assumptions. The first one is that particles with different energies will be released at the same time from the Sun or near the Sun. The second one is that the path lengths for protons with different energies traveling from the Sun to the Earth are the same. The third one is that the pitch angles of first arriving particles are zero, namely that the propagation of particles with different energies is scatter free from the Sun to the Earth. According to VDA, the release times of RSPs seemly support that the RSPs were accelerated by the CME-driven shocks (Reames 2009b). However, statistical results show that for the SEP events with source locations in the well connected region, $E \geq 30$ MeV protons may be mainly accelerated by the concurrent flares (Le et al. 2017; Le & Zhang 2017), suggesting that the real path lengths traveled by particles from the Sun to the Earth should be longer than those obtained by VDA. According to the analysis of the radio emissions, Cane (2003) believed that interplanetary scattering must be occurring, implying that path length traveled by particles from the Sun to the Earth should be longer than the one obtained by VDA.

Wang & Qin (2015) suggested that VDA is only valid with impulsive source duration, low background and weak scattering in interplanetary space or fast diffusion in the solar atmosphere. The low background means that background level is below 0.01% of the peak intensities of the flux (Wang & Qin 2015). The background levels for both $E > 10$ MeV are about 1% of the peak intensities of the flux in the large SEP event that occurred on 2017 September 10, and the situation for $E > 100$ MeV protons is the same as for $E > 10$ MeV protons, suggesting that background is at a medium level and the real path length traveled by particles from the Sun to the Earth should be much longer than the one obtained by VDA (Wang & Qin 2015).

It is more commonly accepted that a perpendicular shock has stronger ability to accelerate particles than a parallel shock (e.g., Tylka et al. 2005; Reames 2012) although some researchers argued that a parallel shock has more ability in accelerating protons than a perpendicular shock (e.g., Lee 2005; Zank et al. 2006). Very recently, a simulation study made by Qin et al. (2018) suggested that stronger acceleration of particles occurs during a perpendicular shock than during a parallel shock. The source location of the SEP event on 2017 September 10 is S06W88, suggesting that only the particles accelerated by the shock driven by the east flank of the CME can be observed by the *GOES* spacecraft. The shock driven by the CME east flank is usually a parallel shock, which is often a weak shock. This kind of shock can hardly accelerate the protons to relativistic energy, implying that RSPs are more likely to be accelerated by the concurrent flare.

Type II radio emission occurs at the local plasma frequency and/or its harmonic, so the frequency of emis-

Table 1 GCS Model Parameters of the CME at Different Times

Longitude (°)	Latitude (°)	Tilt angle (°)	Height (R_s)	Ratio	Half angle (°)	STA time (yyyy/mm/dd hh:mm)	*SOHO* time (yyyy/mm/dd hh:mm)
90	–10	45	2.5	0.6	60	2017/09/10 16:00	2017/09/10 16:00
90	–10	45	3.8	0.6	60	2017/09/10 16:05	2017/09/10 16:00
90	–10	45	5.6	0.6	60	2017/09/10 16:10	2017/09/10 16:12
90	–10	45	13.0	0.6	60	2017/09/10 16:24	2017/09/10 16:42
90	–10	45	15.5	0.6	60	2017/09/10 16:39	2017/09/10 16:54

Table 2 Spheroid Model Parameters of the Shock at Different Times

Longitude (°)	Latitude (°)	Tilt angle (°)	e	κ	Height (R_s)	STA time (yyyy/mm/dd hh:mm)	*SOHO* time (yyyy/mm/dd hh:mm)
95	–8	0	–0.5	0.85	2.3+0.5	2017/09/10 16:00	2017/09/10 16:00
95	–8	0	–0.5	0.85	3.5+0.5	2017/09/10 16:05	2017/09/10 16:00
95	–10	0	–0.5	0.85	5.8+0.15	2017/09/10 16:10	2017/09/10 16:12
95	–10	0	–0.5	0.85	13.7	2017/09/10 16:39	2017/09/10 16:42
95	–10	0	–0.5	0.85	16.5	2017/09/10 16:54	2017/09/10 16:54

Table 3 Characteristic Times of the SEP Event on 2017 September 10

Category	Onset time 1 AU (UT)	Peak time 1 AU (UT)	Traveling time (min)	SRT Sun (ST)
SXR (1–8 Å)	15:35	16:06	8.33	15:26:40[a]
				15:57:40[b]
HXR (100–300 keV)	15:56	16:12	8.33	15:47:40
HXR (300–1000 keV)	15:59:30		8.33	15:51:10
Type III-l burst	15:45		8.33	15:36:40
Type II burst	>16:03		8.33	>15:54:40
CME entered LASCO C2	16:00		8.33	15:51:40
			Path length =1.7 AU	
Electrons (38–53 keV)	16:15±5		38.7	15:36:18±5
Electrons (173–315 keV)	16:10±5		21.3	15:48:42±5
Protons ($E > 30$ MeV)	16:20±5		52.2	15:28:48±5
Protons ($E = 50$ MeV)	16:20±5		45.0	15:35±5
Protons ($E > 100$ MeV)	16:20±5		33.0	15:47±5
Protons ($E > 700$ MeV)	16:15±5		17.3	15:54:42±5
FSMT NM (1 GV)	16:12±1		19.4	15:52:36±1
MGDN NM (2.09 GV)	16:20±1		15.5	16:04:30±1
APTY NM (1 GV)	16:34±1		19.4	16:14:36±1
OULU NM (1 GV)	16:40±1		19.4	16:20:36±1
SOPO NM (1 GV)	16:42±1		19.4	16:22:36±1

Notes: [a] indicates the solar time for start time of the flare; [b] indicates the solar time for peak time of the flare.

sion is indicative of the heliocentric distance at which the radio emission originates. Type II bursts are narrow band radio emissions typically drifting downward in frequency. Drift rates of Type II bursts are indicative of the speed of the shock driven by the associated CME. We can see from Figure 2 that the drift rates of Type II bursts during the early phase are very slow, indicating that the speed of the shock driven by the east flank of the CME is very slow at the early phase, suggesting that the shock driven by the CME east flank is really a weak shock. The enhancement in the flux of $E > 10$ MeV protons was very small when the shock passed the Earth, as shown in Figure 3, indicating that the shock was very weak when it reached the Earth. The shock should be driven by the far east flank of the CME when the shock passed the Earth. This may be the reason why the shock is so weak. It can

be noticed that the fitted speed of the CME by the GCS model is the speed of the CME nose, not the speed of the CME east flank.

Near relativistic electrons can be efficiently accelerated by a perpendicular shock (e.g., Carley et al. 2013; Guo & Giacalone 2010; Kong et al. 2016). However, the shock driven by the CME east flank is a parallel shock, which is not efficient for accelerating electrons, implying that the near relativistic electrons in the SEP event of 2017 September 10 may have been accelerated by the concurrent flare. Solar wind speed is about $550\,\mathrm{km\,s^{-1}}$ before the SEP event, which is shown in Figure 7. The length of the nominal Parker spiral line linking the Sun and the Earth is about 1.3 AU and the estimated longitude of the footpoint of the Parker spiral line on the Sun is about W45 for solar wind speed around $550\,\mathrm{km\,s^{-1}}$. Because the source location of the SEP event is S08W88, it is evident that SEPs observed by the *GOES* spacecraft not only travel along the Parker spiral line, but also must have lateral propagation.

The source locations of two GLE events that occurred on 1982 November 26 and 1982 December 7 are S12W87 and S19W86 respectively. The path lengths for particles traveling from the Sun to the Earth inferred by VDA are 1.96 AU and 1.78 AU respectively for the two GLE events that occurred on 1982 November 26 and 1982 December 7 (Reames 2009a). Based on the assumption of being scatter free, the path length traveled by particles from the Sun to the Earth inferred by VDA should be the shortest one, implying that real path lengths should be longer than 1.96 AU and 1.78 AU respectively for the two GLE events. The longitude of the source location of the SEP event that occurred on 2017 September 10 is W88, which is closer to the west limb of the Sun than those of the two SEP events that occurred on 1982 November 26 and 1982 December 7, suggesting that the path length traveled by protons from the Sun to the Earth for the SEP event of 2017 September 10 should be longer than 1.7 AU.

According to the path length traveled by particles and the onset times for particles with different energies, the derived SRTs for particles with different energies are different, which can be seen from Table 3. We can also see from Table 3 that SRTs with $E > 30$, 50 and 100 MeV occurred during the impulsive phase of the X8.2 flare. In addition, the SRT with $E > 100$ MeV protons is earlier than the solar time of the Type II radio burst, and the SRTs with $E > 30$ MeV and $E > 50$ MeV protons are much earlier than the solar time of the Type II radio burst, suggesting that the first arriving $E > 30$, $E > 50$ and $E > 100$ MeV protons should have been accelerated by the concurrent flare.

The onset times for both $E > 30$ MeV protons and $E > 100$ MeV protons are 16:20 UT $\pm$5 min, indicating that the time difference between the onset times for $E > 30$ MeV protons and $E > 100$ MeV protons should not exceed 10 min. However, the derived SRT of $E > 30$ MeV protons is 19.2 min earlier than that of $E > 100$ MeV protons, suggesting that the release time for $E > 30$ MeV protons is at least 9.2 min earlier than that for $E > 100$ MeV protons, namely that protons with lower energy may leave the Sun earlier than those with higher energy.

The earliest onset time of RSPs is observed by the FMST NM. The derived SRT of RSPs observed by FMST NM is 15:52$\pm$1 min ST, which is earlier than the start time of the Type II radio burst. The time that the CME just entered the LASCO C2 view field is consistent with the time when first arriving RSPs reached the Earth and any interaction of the CME with the structures higher in the corona could not have happened and could not have played a role in the acceleration of the first arriving high energy protons. We can also see from Table 3 that the onset times of RSPs observed by several NMs were later than the peak time of soft X-ray (SXR) flux, and also later than the first peak time of 100–300 keV HXR flux, suggesting that the protons accelerated by the concurrent flare may be further accelerated by the CME-driven shock to higher energy.

SRTs estimated for different energy protons are based on the assumption that the path length traveled by protons is the same as that traveled by electrons. However, the path length traveled by protons is usually longer than that traveled by electrons. As a result, the SRTs for protons with different energies should be earlier than those listed in Table 3. This will further support that the first arriving protons are accelerated by the concurrent flare.

According to the data analyses and the discussion above, the results can be summarized as below:

(1) The cosmic rays are highly anisotropic at the early phase and a few protons have energy greater than 1.64 GeV. Both the first arriving RSPs and non-RSPs may be accelerated by the concurrent flare, and the

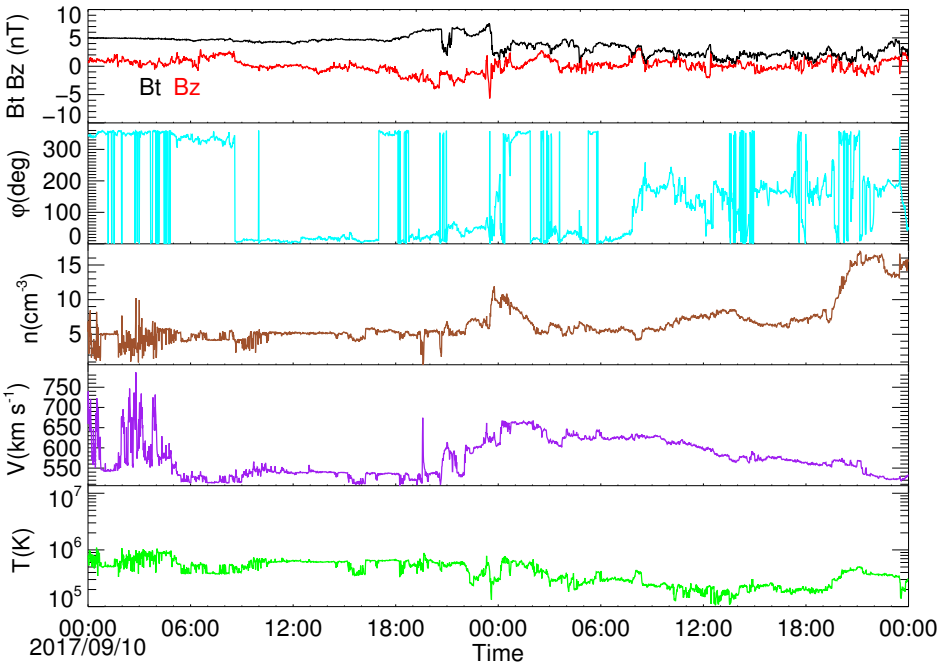

Fig. 7 Solar wind parameters during 2017 September 10-11 observed by *DSCOVR*. From *top* to *bottom*, the panels indicate interplanetary magnetic field (IMF) with a *black line* for the total IMF and a *red line* for the z-component of IMF, azimuth ϕ, proton densities, solar wind speed and proton temperature respectively.

first near relativistic electrons may also be accelerated by concurrent flares.

(2) The release times of protons with different energies may be different. The protons with lower energy may be released earlier than those with higher energy.

(3) The estimated averaged CME speed was about 2808.8 km s^{-1} in the LASCO C2 and C3 view field, while the CME-driven shock speed was about 2933.5 km s^{-1} in the LASCO C2 and C3 view field. Protons accelerated by the concurrent flare may be further accelerated by the CME-driven shock.

(4) The interaction of the CME with structures higher in the corona could not have played a role in accelerating the first arriving high energy protons.

Acknowledgements We are very grateful to the anonymous referee for her/his reviewing of the paper and for helpful suggestions. We also thank the scientific editor for his useful comments. We are grateful to *SOHO*, *STEREO*, *GOES*, *ACE*, *FERMI* and NMDB for making their data available online. This work was jointly funded by the National Natural Science Foundation of China (Grant Nos. 41674166, 41074132, 41274193 and 41304144) and the National Standard Research Program (Grant 200710123).

References

Aurass, H., Mann, G., Rausche, G., & Warmuth, A. 2006, A&A, 457, 681

Bazilevskaya, G. A. 2009, Advances in Space Research, 43, 530

Bieber, J. W., Dröge, W., Evenson, P. A., et al. 2002, ApJ, 567, 622

Brueckner, G. E., Howard, R. A., Koomen, M. J., et al. 1995, Sol. Phys., 162, 357

Cane, H. V., Erickson, W. C., & Prestage, N. P. 2002, Journal of Geophysical Research (Space Physics), 107, 1315

Cane, H. V. 2003, ApJ, 598, 1403

Cane, H. V., & Lario, D. 2006, Space Sci. Rev., 123, 45

Cane, H. V., Mewaldt, R. A., Cohen, C. M. S., & von Rosenvinge, T. T. 2006, Journal of Geophysical Research (Space Physics), 111, A06S90

Cane, H. V., Richardson, I. G., & von Rosenvinge, T. T. 2010, Journal of Geophysical Research (Space Physics), 115, A08101

Carley, E. P., Long, D. M., Byrne, J. P., et al. 2013, Nature Physics, 9, 811

Cliver, E. W., & Ling, A. G. 2009, ApJ, 690, 598
Grechnev, V. V., Kurt, V. G., Chertok, I. M., et al. 2008, Sol. Phys., 252, 149
Grechnev, V. V., Kiselev, V. I., Meshalkina, N. S., & Chertok, I. M. 2015, Sol. Phys., 290, 2827
Guo, F., & Giacalone, J. 2010, ApJ, 715, 406
Kahler, S. W., Aurass, H., Mann, G., & Klassen, A. 2007, ApJ, 656, 567
Klein, K.-L., Masson, S., Bouratzis, C., et al. 2014, A&A, 572, A4
Kong, X., Chen, Y., Guo, F., et al. 2016, ApJ, 821, 32
Kouloumvakos, A., Nindos, A., Valtonen, E., et al. 2015, A&A, 580, A80
Le, G.-M., Tang, Y.-H., & Han, Y.-B. 2006, ChJAA (Chin. J. Astron. Astrophys.), 6, 751
Le, G.-M., Li, P., Yang, H.-G., et al. 2013, RAA (Research in Astronomy and Astrophysics), 13, 1219
Le, G., Yang, X., Ding, L., et al. 2014, Ap&SS, 352, 403
Le, G.-M., Li, C., Tang Y., et al. 2016, RAA (Research in Astronomy and Astrophysics), 16, 14
Le, G.-M., Li, C., & Zhang, X.-F. 2017, RAA (Research in Astronomy and Astrophysics), 17, 073
Le, G.-M., & Zhang, X.-F. 2017, RAA (Research in Astronomy and Astrophysics), 17, 123
Lee, M. A. 2005, ApJS, 158, 38
Li, C., Dai, Y., Vial, J.-C., et al. 2009, A&A, 503, 1013
Li, C., Tang, Y. H., Dai, Y., Fang, C., & Vial, J.-C. 2007a, A&A, 472, 283
Li, C., Tang, Y. H., Dai, Y., Zong, W. G., & Fang, C. 2007b, A&A, 461, 1115
Lin, R. P., Krucker, S., Hurford, G. J., et al. 2003, ApJ, 595, L69
Masson, S., Klein, K.-L., Bütikofer, R., et al. 2009, Sol. Phys., 257, 305
Meegan, C., Lichti, G., Bhat, P. N., et al. 2009, ApJ, 702, 791
Mewaldt, R. A., Cohen, C. M. S., Haggerty, D. K., et al. 2003, International Cosmic Ray Conference, 6, 3313
Miroshnichenko, L. I., ed. 2001, Astrophysics and Space Science Library, 260, Solar Cosmic Rays (Kluwer Academic Publishers)
Miroshnichenko, L. I., Klein, K.-L., Trottet, G., et al. 2005a, Advances in Space Research, 35, 1864
Miroshnichenko, L. I., Klein, K.-L., Trottet, G., et al. 2005b, Journal of Geophysical Research (Space Physics), 110, A11S90
Pérez-Peraza, J., Vashenyuk, E. V., Miroshnichenko, L. I., Balabin, Y. V., & Gallegos-Cruz, A. 2009, ApJ, 695, 865
Qin, G., Kong, F.-J., & Zhang, L.-H. 2018, arXiv:1802.08367
Reames, D. V. 2009a, ApJ, 706, 844
Reames, D. V. 2009b, ApJ, 693, 812
Reames, D. V. 2012, ApJ, 757, 93
Simnett, G. M. 2006, A&A, 445, 715
Thernisien, A. F. R., Howard, R. A., & Vourlidas, A. 2006, ApJ, 652, 763
Thernisien, A., Vourlidas, A., & Howard, R. A. 2009, Sol. Phys., 256, 111
Tylka, A. J., Cohen, C. M. S., Dietrich, W. F., et al. 2005, ApJ, 625, 474
Tylka, A. J., Cohen, C. M. S., Dietrich, W. F., et al. 2003, International Cosmic Ray Conference, 6, 3305
Wang, Y., & Qin, G. 2015, ApJ, 799, 111
Zank, G. P., Li, G., Florinski, V., et al. 2006, Journal of Geophysical Research (Space Physics), 111, A06108